FEBS Letters 588 (2014) 4665–4671

journal homepage: www.FEBSLetters.org

DNA methylation dynamics of a maternally methylated DMR in the mouse *Dlk1–Dio3* domain

Tie-Bo Zeng, Hong-Juan He, Zheng-Bin Han, Feng-Wei Zhang, Zhi-Jun Huang, Qi Liu, Wei Cui, Qiong Wu *

School of Life Science and Technology, State Key Laboratory of Urban Water Resources and Environment, Harbin Institute of Technology, Harbin 150080, Heilongjiang, China

ARTICLE INFO

Article history:
Received 22 September 2014
Revised 26 October 2014
Accepted 30 October 2014
Available online 11 November 2014

Edited by Takashi Gojobori

Keywords:
DNA methylation
Genomic imprinting
Differentially methylated region
CCCTC-binding factor
Dlk1–Dio3 domain

ABSTRACT

The mouse delta-like homolog 1 and type III iodothyronine deiodinase (*Dlk1–Dio3*) imprinted domain contains three known paternally methylated differentially methylated regions (DMRs): intergenic DMR (IG-DMR), maternally expressed 3-DMR (*Gtl2*-DMR), and *Dlk1*-DMR. Here, we report the first maternally methylated DMR, CpG island 2 (CGI-2), is located approximately 800 bp downstream of miR-1188. CGI-2 is highly methylated in sperm and oocytes, de-methylated in pre-implantation embryos, and differentially re-methylated during post-implantation development. CGI-2, similarly to *Gtl2*-DMR and *Dlk1*-DMR, acquires differential methylation prior to embryonic day 7.5 (E7.5). Both H3K4me3 and H3K9me3 histone modifications are enriched at CGI-2. Furthermore, CCCTC-binding factor (CTCF) binds to both alleles of CGI-2 *in vivo*. These results contribute to the investigation of imprinting regulation in this domain.

1. Introduction

Imprinted genes exhibit allele-specific transcription in a parent-of-origin dependent manner [1]. Most known imprinted genes are clustered and co-regulated by regional control elements that are differentially methylated on the two parental chromosomes [2]. Identification of differentially methylated regions (DMRs) has greatly contributed to our understanding of imprinting regulation [3]. Allele-specific DNA methylation can be established either in the germline or post-fertilization (defined as germline and somatic DMRs, respectively) [4]. The *Dlk1–Dio3* imprinted domain on mouse chromosome 12qF1 contains three paternally expressed protein-coding genes, multiple maternally expressed long non-coding RNA genes, and numerous miRNAs and snoRNAs [5–10]. The expression of long non-coding RNAs and lots of miRNAs clustered in this domain is aberrantly silenced in most mouse induced pluripotent stem (iPS) cells, and is predictive for their developmental potential [11–13]. There are three known paternally methylated DMRs (IG-DMR, *Gtl2*-DMR and *Dlk1*-DMR) [14]. IG-DMR is a germline DMR that functions as the imprinting control region [15,16], *Gtl2*-DMR is a somatic DMR that spans the *Meg3*/*Gtl2* promoter [17,18].

A previous study found that, when received a randomly integrating adeno-associated virus (AAV) vector, mice developed hepatocellular carcinoma (HCC) that contained integrated vector genomes within the *Dlk1–Dio3* domain. All four insertion sites mapped to a 6-kb region, including the miR-341 locus [19]. Genes adjacent and telomeric to the AAV vector integration sites were up-regulated in all tumor samples examined [20]. Another study using a modified *sleeping beauty* transposon system also found this locus is involved in HCC [21]. Transcriptome analysis showed that transposon integration near miR-341 led to overexpression of numerous long non-coding RNAs and miRNAs in this domain [22]. These results suggest that insertional mutagenesis around miR-341 can cause overexpression of upstream or downstream genes. However, the underlying mechanism is not very clear. We hypothesized that there might be some unknown regulatory sequences in close proximity to miR-341. Interestingly, a previous study suggested a potential DMR is located near miR-341 (and upstream of *Rtl1* on the reverse strand) [23]. In this study, we focused on two small predicted CpG islands (CGI-1 and CGI-2) in intron 2 of *Meg8*. While CGI-1 (chr12:110849680-110849939, mm9) spans miR-341, CGI-2 (chr12:110850932-110851278) is located ~800 bp downstream of miR-1188 (Fig. 1). We performed detailed methylation analysis of CGI-1 and CGI-2 throughout mouse embryonic development, and found that CGI-2 is a maternally methylated somatic DMR.

2. Materials and methods

2.1. Ethics statement

All animal experiments were carried out according to the guidelines for the care and use of experimental animals approved by the National Institutes for Food and Drug Control of China (http://

* Corresponding author. Fax: +86 451 86403181.
E-mail address: kigo@hit.edu.cn (Q. Wu).

http://dx.doi.org/10.1016/j.febslet.2014.10.038
0014-5793/

www.nicpbp.org.cn/sydw/CL0249/2730.html). Purchased mice were housed in standard plastic cages with a 12-h light–dark cycle in the Center for Experimental Animal of Harbin Institute of Technology. Pregnant mice were sacrificed by cervical dislocation to obtain mouse embryos from morula to E18.5. This study had received the approval to sacrifice the pregnant mice and use their embryos from the Ethical Committee of Harbin Institute of Technology.

2.2. Mouse samples

6–8 weeks old C57BL/6 J (BL6) and ICR (also called CD-1) mice were purchased from Vital River Laboratory Animal Technology Co. Ltd (Beijing, China). Early embryos and fetal tissues of F1 hybrids were obtained by reciprocally crossing BL6 and ICR mice. Breeding was performed overnight. The presence of a vaginal plug in the morning was defined as embryonic day 0.5 (E0.5). Spermatozoa were obtained from the vas deferens of adult male BL6 and ICR mice. MII oocytes were collected from the ovaries of superovulated 6–8 weeks old female BL6 and ICR mice, and washed in CZB medium containing hyaluronidase (Sigma–Aldrich) to remove the cumulus cells. Tissues used for methylation analysis and ChIP assays were isolated from E15.5 BIF1 (BL6♀ × ICR♂) and E18.5 IBF1 (ICR♀ × BL6♂) embryos.

2.3. DNA extraction and bisulfite sequencing analysis

Genomic DNA samples were isolated from E15.5 and E18.5 tissues and mature sperm by standard method using proteinase K (Roche, Mannheim, Germany) digestion, RNase A (Fermentas) treatment, and followed by phenol/chloroform extraction and ethanol precipitation. Bisulfite modification of the isolated DNA was performed using the EZ DNA methylation-Gold kit (Zymo Research, cat# D5005, Orange, CA, USA) according to the manufacturer's instructions. Bisulfite-treated samples were amplified by nested PCR using Zymo*Taq*™ DNA Polymerase (Zymo Research, cat# E2001). Primer sequences, SNP information and PCR conditions are listed in Table S1. PCR products were subcloned into pMD19 T-Vector (TaKaRa, cat# 3271, Dalian, China). Plasmids were isolated from selected clones and sequenced by the ABI PRISM 3500 Genetic Analyzer (Applied Biosystems, CA, USA) using a BigDye® Terminator v3.1 Cycle Sequencing Kit (Applied Biosystems).

2.4. Methylation analysis in early embryos

Before subjected to bisulfite treatment, numerous oocytes or several early embryos at each of the stages were pooled, the numbers are as follows (partially referred to [18]): ~200 ICR oocytes, ~140 BL6 oocytes, eleven BIF1 or thirteen IBF1 morulae, eight BIF1 or six IBF1 blastocysts, four BIF1 or five IBF1 whole embryos at E5.5, two BIF1 or three IBF1 whole embryos at E6.5, one BIF1 or two IBF1 whole embryos at E7.5. BIF1 and IBF1 embryos were separately analyzed at once. All pooled samples were directly subjected to proteinase K digestion and bisulfite treatment using the EZ DNA methylation-direct kit (Zymo Research, cat# D5020). PCR and cloning procedures are the same as described above.

2.5. Chromatin immunoprecipitation (ChIP) assays

ChIP experiments were performed using a ChIP assay kit (Upstate Biotechnology, cat# 17-295) according to the manufacturer's instructions. Briefly, ~50 mg liver or placenta tissue was homogenized in 1 × PBS containing protease inhibitors (1 mM PMSF, 1 μg/μl pepstatin, and 1 μg/μl aprotinin), treated with formaldehyde to final concentration of 1% at 37 °C for 10 min, and resuspended in SDS lysis buffer. The cross-linked DNA was sheared by sonication to 200–1000 bp in length. After centrifugation, the whole-cell extract was diluted and precleared with protein A agarose slurry to reduce non-specific background. For immunoprecipitation, 5 μg of anti-Tri-Methyl-Histone H3 (Lys4) (Cell Signaling Technology, #9751), 5 μg of anti-Histone H3 (tri methyl K9) (Abcam, ab8898), 5 μg of anti-CTCF (Upstate Biotechnology, 07-729) or 5 μg of normal rabbit IgG was added, and the mixture was incubated overnight at 4 °C with rocking. Next morning, the immune complexes were collected, washed in a series of buffers and reverse cross-linked. DNA was purified through phenol/chloroform extraction and used as templates for PCR amplification. PCR products were analyzed by running on 1.5% agarose gel with ethidium bromide staining, purified and directly sequenced.

3. Results

3.1. Methylation analysis of CGI-1 and CGI-2 in mid to late gestation somatic tissues

To find CGIs in the vicinity of mouse miR-341 and miR-1188, the online software CpG Island Searcher (http://cpgislands.usc.edu/) [24] was used with the following parameters: minimum length 200 bp, GC content greater than 50%, and ratio CpG observed/expected greater than 0.60. As a result we found two CGIs, named CGI-1 and CGI-2 (Fig. 1). To determine the methylation patterns of CGI-1 and CGI-2, bisulfite sequencing analysis

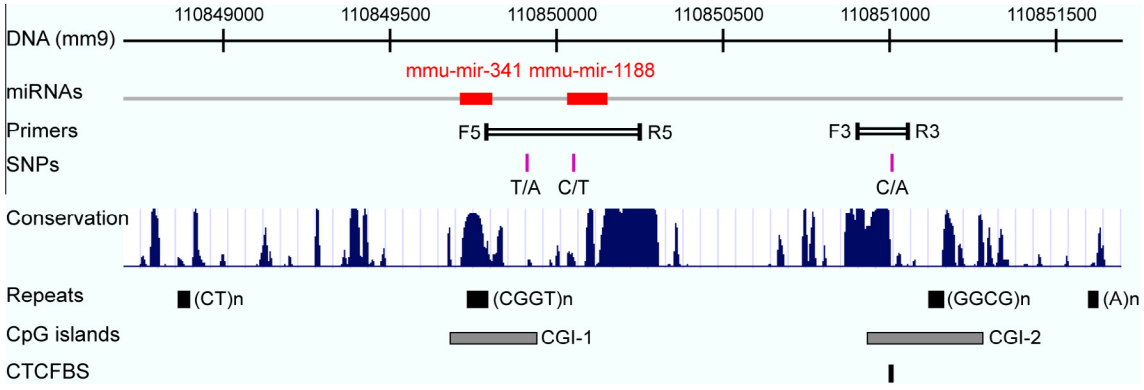

Fig. 1. Schematic representation of the loci of miR-341/miR-1188 and CGI-1/CGI-2. The precursor sequences of miR-341 and miR-1188 are located 227 bp apart. While CGI-1 overlaps miR-341, CGI-2 is located ~800 bp downstream of miR-1188. SNPs T/A and C/A are used to distinguish the two parental alleles of CGI-1 and CGI-2, respectively. CGI-1 contains (CGGT)n tandem repeats, and CGI-2 contains (GGCG)n tandem repeats. The conservation chromatogram was downloaded from the UCSC Genome Browser. Primers F3/R3 flank the third predicted CTCF binding site within CGI-2.

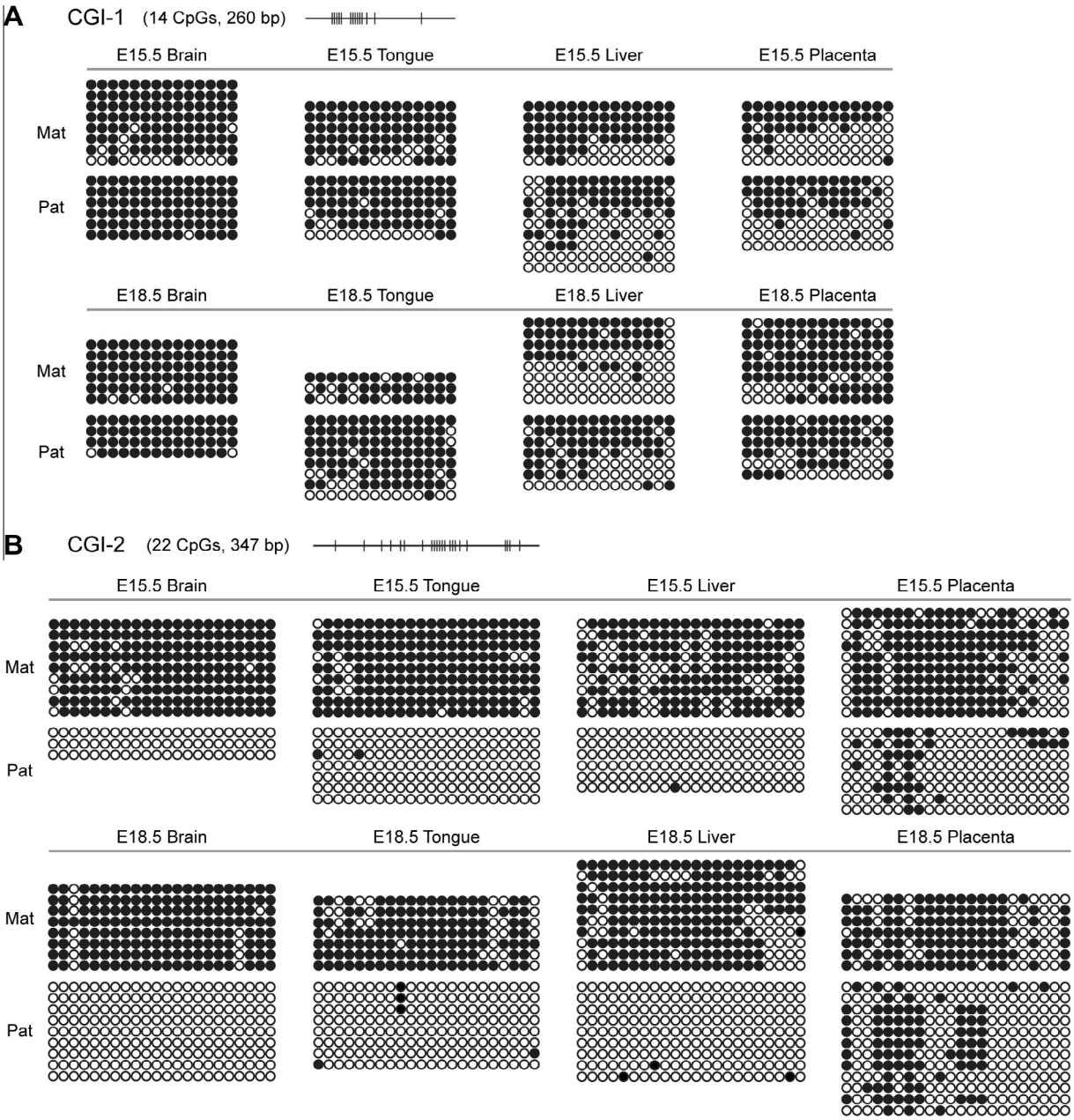

Fig. 2. Bisulfite sequencing analysis of CGI-1 (A) and CGI-2 (B) in E15.5 and E18.5 tissues. The analyzed region of CGI-1 and CGI-2 contains 14 and 22 CpG dinucleotides, respectively. Each CpG dinucleotide is represented with a circle. Each row of circles represents an individual clone sequenced. Black and white circles represent methylated and unmethylated CpGs, respectively. SNPs used to discriminate the maternal (Mat) and paternal (Pat) alleles are shown in Fig. 1.

was performed on BIF1 E15.5 and IBF1 E18.5 tissues. At least one single nucleotide polymorphism (SNP) can be found for CGI-1 or CGI-2, allowing the two parental alleles to be distinguished. The results showed that CGI-1 was hypermethylated on both paternal and maternal alleles in brain and tongue at E15.5 and E18.5; the methylation levels in liver and placenta were lower than that in brain and tongue, but CGI-1 was not a allele-specific DMR (Fig. 2A). For CGI-2, we observed striking methylation differences between the two parental alleles in brain, tongue and liver at E15.5 and E18.5. CGI-2 was hypermethylated on the maternally inherited chromosomes, but paternally unmethylated (Fig. 2B). The methylation level on the paternal allele of CGI-2 increased in placenta, indicative of tissue-specific methylation status. These results suggest that CGI-2 is a maternally methylated DMR in somatic tissues, while CGI-1 is not.

3.2. Methylation analysis of CGI-1 and CGI-2 in mouse gametes, pre- and post-implantation embryos

To determine if the maternal allele-specific methylation of CGI-2 is acquired during gametogenesis, we analyzed the methylation status of this region in mature sperm and MII oocytes. The results showed that CGI-2 was highly methylated in both sperm and oocytes obtained from BL6 or ICR mice (Fig. 3), indicating CGI-2 acquires its differential methylation after fertilization. CGI-1 was also methylated in both sperm and oocytes. We further investigated the methylation dynamics of CGI-1 and CGI-2 in pre- and post-implantation embryos. Bisulfite sequencing analysis was performed on reciprocal crosses between BL6 and ICR mice. During the pre-implantation development, there is a known genome-wide demethylation process [25,26]. Consistent with this, CGI-1 and

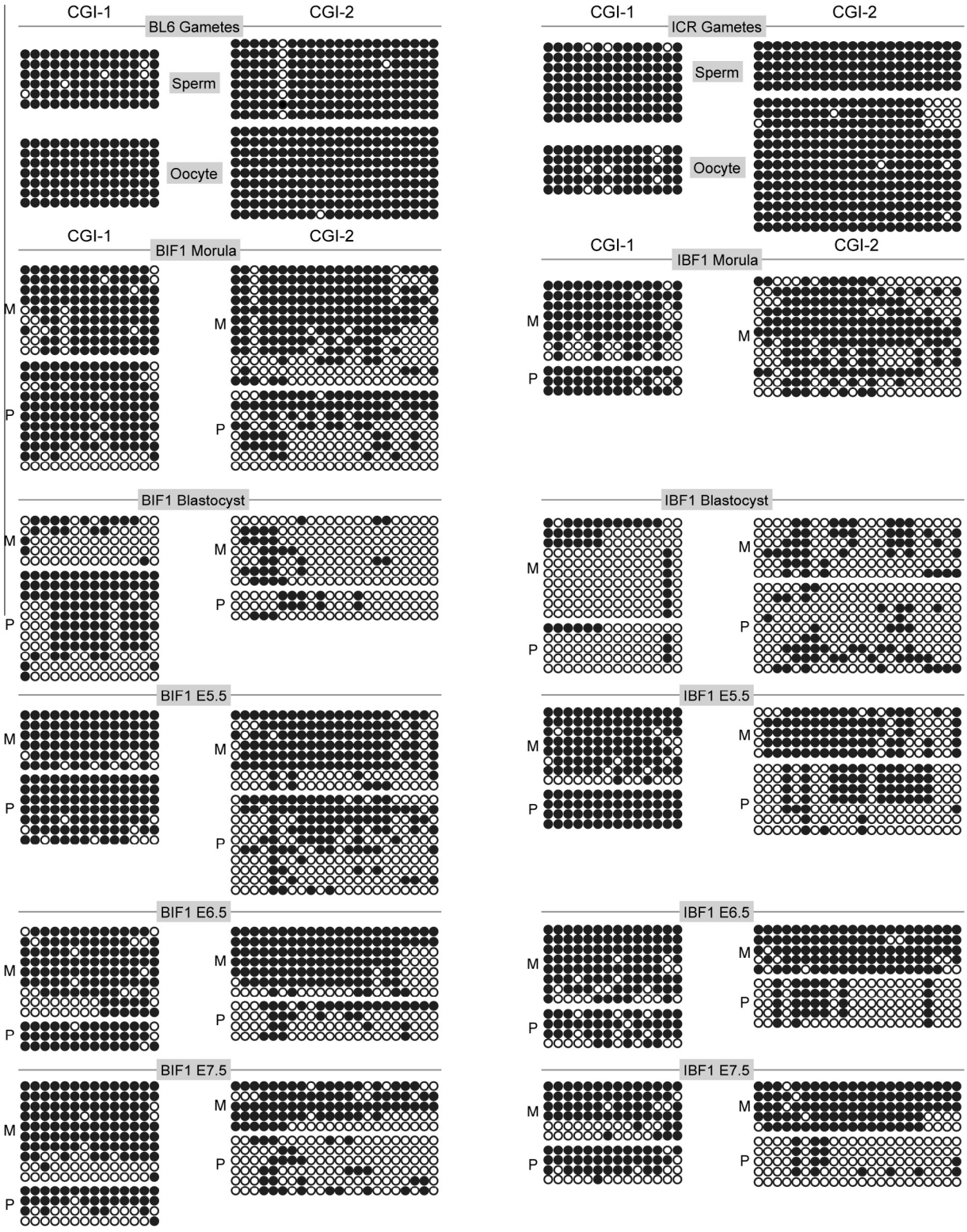

Fig. 3. Bisulfite sequencing analysis of CGI-1 and CGI-2 in mouse gametes, pre- and post-implantation embryos on reciprocal crosses between BL6 and ICR mice. CGI-1 and CGI-2 are highly methylated in sperm and oocytes, demethylated in pre-implantation embryos, and re-methylated after implantation. The paternal allele of CGI-2 is firstly re-methylated, and then demethylated from E5.5 to E7.5. Details are the same as described in the legend of Fig. 2.

CGI-2 were hypomethylated in blastocysts, and the methylation levels of CGI-1 and CGI-2 in morulae were lower than in gametes, a demethylation process had happened (Fig. 3). CGI-2 was not a DMR in pre-implantation embryos.

Upon implantation, global re-methylation begins [25,26]. At the E5.5 stage, the maternal allele of CGI-2 was largely re-methylated, and it retained DNA methylation from E5.5 to E7.5; the paternal allele of CGI-2 was also partly re-methylated. Interestingly, from

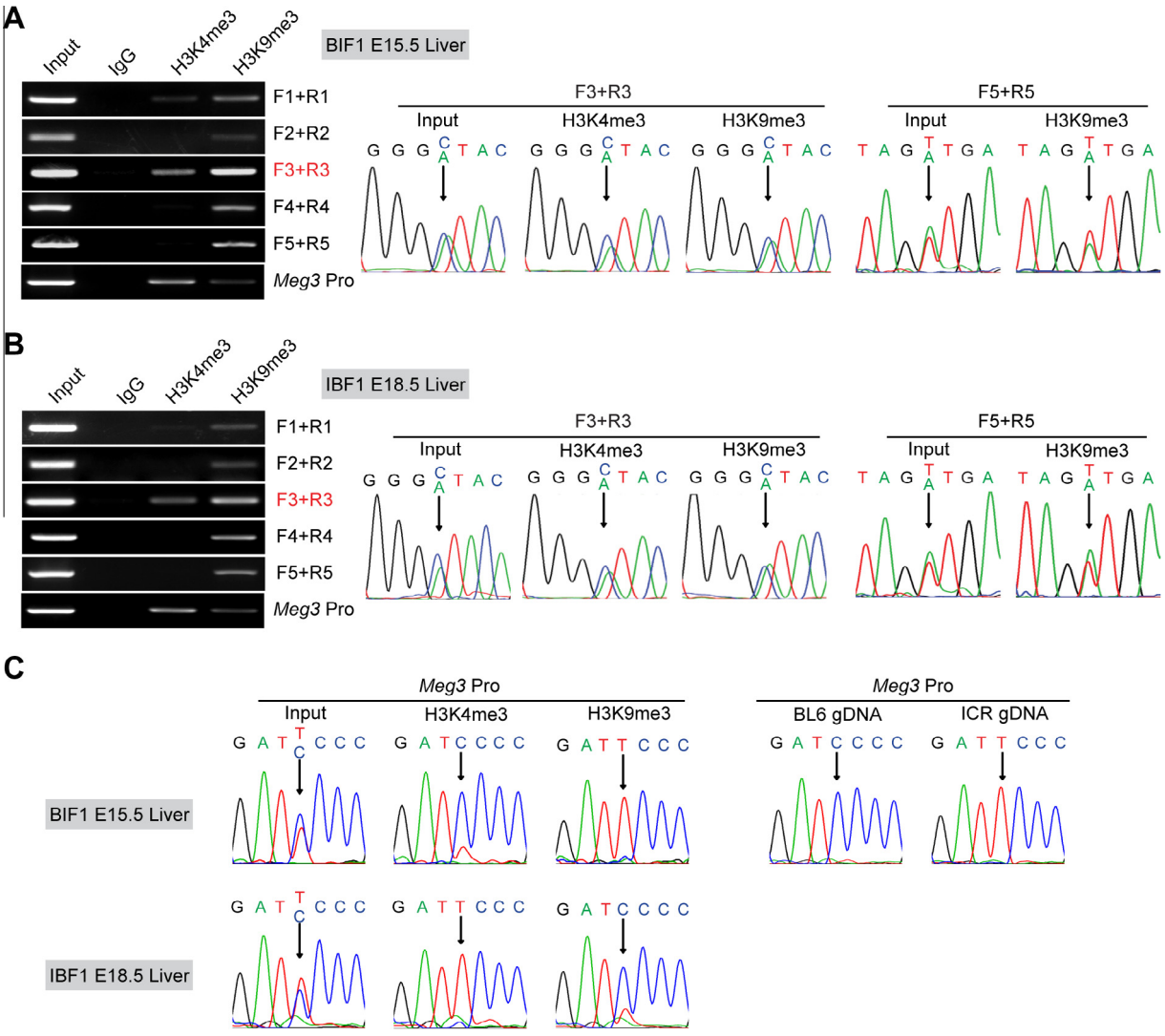

Fig. 4. Analysis of modified histones H3K4me3 and H3K9me3 at CGI-2 and its adjacent regions. (A and B) ChIP assays were performed in BIF1 E15.5 and IBF1 E18.5 liver. The immunoprecipitated DNA was analyzed by five PCR primer pairs shown in Figs. 1 and S1. Only the amplicons of primers F3/R3 and F5/R5 contain a SNP, and were directly sequenced. (C) The *Meg3* promoter was marked by maternal H3K4me3 and paternal H3K9me3 as expected.

E5.5 to E7.5, the methylation level on the paternal allele of CGI-2 was gradually decreasing; CGI-2 acquired its differential methylation pattern by approximately E7.5 (Fig. 3). For CGI-1, hypermethylation was always observed on both paternal and maternal alleles from E5.5 to E7.5 (Fig. 3). CGI-1 and CGI-2 are located only ~1 kb apart, but show different methylation dynamics. Altogether, these results suggest that CGI-2 undergoes a complex demethylation and re-methylation process during pre- and post-implantation development, and acquires differential methylation prior to E7.5.

3.3. Analysis of histone H3K4me3 and H3K9me3 modifications

A previous study identified an overlapping pattern of histone H3K4me3 and H3K9me3 modifications in somatic tissue at 11 potential new DMRs, including the locus of CGI-2 (upstream of *Rtl1*) [23], but the allelic specificity of these permissive and repressive histone modifications was not determined. To find out how histone H3K4me3 and H3K9me3 are enriched at CGI-2 and its adjacent regions, we performed ChIP assays in BIF1 E15.5 and IBF1 E18.5 liver. The immunoprecipitated DNA was analyzed by five PCR primer pairs (Figs. 1 and S1B, see text below). We found that both histones H3K4me3 and H3K9me3 were indeed enriched at CGI-2 (Fig. 4A and B). Weak enrichment of histone H3K4me3 was also found using primers F1/R1. Extensive histone H3K9me3 enrichments were observed in all analyzed regions. Only the amplicons of primers F3/R3 and F5/R5 contain a SNP. Directly sequencing the PCR products showed that all these enrichments were biallelic (Fig. 4A and B). As previously reported [27], histone H3K4me3 and H3K9me3 were enriched on the maternal and paternal allele of *Meg3* promoter, respectively (Fig. 4C).

3.4. CTCF binds to CGI-2 in vivo

CCCTC-binding factor (CTCF) is known to bind many DMRs and play a role in imprinting regulation [28–32]. Next, we examined if CTCF binds to the differentially methylated CGI-2. When searching the publicly available CTCF ChIP-seq data from the human ENCODE project [33–35], we found four CTCF binding peaks around human miR-1188 (Fig. S1A). Sequence alignments showed all CTCF binding sites are conserved between human and mouse. The precise binding motifs were identified by the in silico CTCFBS prediction tool [36] (http://insulatordb.uthsc.edu/storm.php) (Fig. S1C). CTCFBS#3 is located in CGI-2. ChIP assays were performed in mouse tissues using a polyclonal CTCF antibody, with PCR primers

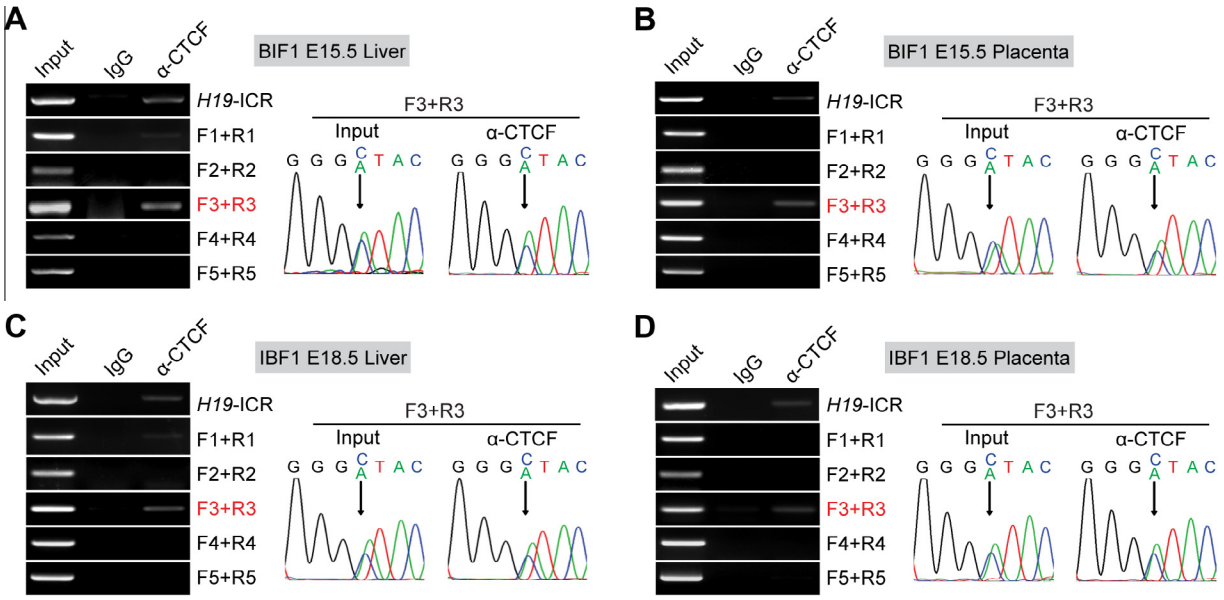

Fig. 5. CTCF binds to CGI-2 *in vivo*. DNA immunoprecipitated by a polyclonal CTCF antibody was analyzed by PCR primers flanking the four predicted CTCF binding sites. Directly sequencing the products of primers F3/R3 showed the binding of CTCF at CGI-2 is biallelic. The *H19*-ICR was used as a positive control, but it does not contain a SNP.

flanking each predicted CTCF binding site (Fig. S1B). We found that in both liver and placenta, enrichment of CTCF could only be detected by primers F3/R3, demonstrating CTCF binds to CGI-2 *in vivo* (Fig. 5). The products of primers F3/R3 were directly sequenced. Both C and A alleles were detected in the input and immunoprecipitated DNA, indicating the binding of CTCF is biallelic. *H19*-ICR was used as a positive control which indeed binds CTCF, but it does not contain a SNP.

4. Discussion

In this study, we found the first maternally methylated DMR named CGI-2 in the *Dlk1–Dio3* imprinted domain, and determined its methylation dynamics in pre- and post-implantation embryos. CGI-2 is highly methylated in both sperm and oocytes, demethylated in pre-implantation embryos, and differentially re-methylated during post-implantation development. The other two somatic DMRs (*Gtl2*-DMR and *Dlk1*-DMR) in this domain are unmethylated in sperm, oocytes and blastocysts, and acquire differential methylation after implantation [17,18,37]. Maternal allele-specific DNA methylation is established at CGI-2 prior to E7.5, incidentally at around the same time as the *Gtl2*-DMR [17,18] and *Dlk1*-DMR [37] which acquire paternal allele-specific DNA methylation at E6.5, indicating the acquisition of allele-specific DNA methylation at these secondary DMRs might be coordinately regulated.

The imprinting analysis using primers F5/R5 and F3/R3 showed that all the transcriptional activities are restricted to the maternally inherited chromosome (Fig. S2), in contrast to the maternal allele-specific DNA methylation of CGI-2. We cannot exclude the possibility that CGI-2 may be involved in regulating gene expression on the maternal allele without necessarily affecting imprinting, but for most, if not all, of known DMRs to date, it is usually the unmethylated allele that play a critical role in imprinting regulation [1,2], so the paternally unmethylated CGI-2 is more likely to have a function on the paternally inherited chromosome. Like IG-DMR [16,38] and *Gtl2*-DMR [39], knockout mouse lines need to be created to explore the target(s) and function of CGI-2. When the maternal IG-DMR was deleted, a maternal to paternal epigenotype switch was observed: *Dlk1*, *Rtl1* and *Dio3* are expressed whereas *Gtl2* and other non-coding RNA genes are silenced on the maternally inherited chromosome, and the maternal *Gtl2*-DMR is hypermethylated [16]. It will be interesting to find out whether CGI-2 loses its differential methylation in IG-DMR knockout mice, or whether IG-DMR acts hierarchically to regulate the methylation status of CGI-2.

At the E5.5 stage, the maternal allele of CGI-2 is re-methylated, *de novo* methylation machinery should have been recruited to CGI-2 and be responsible for it. However, the paternal allele of CGI-2 is not fully re-methylated and further demethylated from E5.5 to E7.5, there may be some unknown pre-existing epigenetic marks that resistant to the *de novo* methylation machinery. In the bisulfite sequencing results, there were always some hypomethylated individual clones derived from the maternal or paternal allele of CGI-1, this is similar to the *Dlk1*-DMR which was recently shown to display high level of hemimethylation [37], the underlying mechanism is not very clear.

CGI-1 and CGI-2 are located ~1 kb apart, and the primer pairs F3/R3 and F5/R5 are very close (Fig. 1). CGI-1 is not a DMR, so it can be easy to understand the enrichment of histone H3K9me3 at CGI-1 is biallelic, but the biallelic enrichment of histones H3K4me3 and H3K9me3 at the differentially methylated CGI-2 is confusing. In the ChIP assays, the cross-linked DNA was sheared by sonication to 200–1000 bp in length. It is very likely that the potentially existed allele-specific histone H3K9me3 at CGI-2 cannot be distinguished from the biallelic histone H3K9me3 at CGI-1. However, this cannot explain the biallelic enrichment of histone H3K4me3 at CGI-2, because no histone H3K4me3 was found at CGI-1 by primers F5/R5 (Fig. 4). While maternal allele-specific histone H3K4me3 can be detected on the *Meg3* promoter as expected, the biallelic enrichment of histone H3K4me3 at CGI-2 should be the case, although its potential significance is hard to consider.

The CTCF binding motif in CGI-2 actually contains no CpG dinucleotide (Fig. S1C), this may partially explain why the differential methylation of CGI-2 does not influence the binding of CTCF. A previous study identified a conserved cluster of CTCF binding sites in the region ~75 kb upstream of *Dlk1* in mouse liver, and demonstrated CTCF binds to site #1 in a biallelic manner [40]. It remains to be elucidated whether these biallelic CTCF binding can participate in the imprinting regulation in this domain.

In summary, CGI-2 is a maternally methylated somatic DMR. The methylation landscape of CGI-2 changes dynamically during pre- and post-implantation development. CGI-2 acquires differential methylation prior to E7.5. Both histones H3K4me3 and H3K9me3 are enriched at CGI-2. CTCF binds to both alleles of CGI-2 *in vivo*. The target(s) and function of CGI-2 remain to be further investigated.

Conflict of interest

The authors declare that they have no conflicts of interest.

Acknowledgments

We would like to thank You-Peng Qu for technical support with DNA sequencing. This work was supported by the National Natural Science Foundation of China (Nos. 31171383, 31100934, 31371478 and 31100928), and the Special Financial Grant from the China Postdoctoral Science Foundation (No. 2013T60353).

Appendix A. Supplementary data

Supplementary data associated with this article can be found, in the online version, at http://dx.doi.org/10.1016/j.febslet.2014.10.038.

References

[1] Barlow, D.P. (2011) Genomic imprinting: a mammalian epigenetic discovery model. Annu. Rev. Genet. 45, 379–403.
[2] Edwards, C.A. and Ferguson-Smith, A.C. (2007) Mechanisms regulating imprinted genes in clusters. Curr. Opin. Cell Biol. 19, 281–289.
[3] Ferguson-Smith, A.C. (2011) Genomic imprinting: the emergence of an epigenetic paradigm. Nat. Rev. Genet. 12, 565–575.
[4] Bartolomei, M.S. and Ferguson-Smith, A.C. (2011) Mammalian genomic imprinting. Cold Spring Harbor Perspect. Biol. 3.
[5] da Rocha, S.T., Edwards, C.A., Ito, M., Ogata, T. and Ferguson-Smith, A.C. (2008) Genomic imprinting at the mammalian Dlk1–Dio3 domain. Trends Genet. 24, 306–316.
[6] Hagan, J.P., O'Neill, B.L., Stewart, C.L., Kozlov, S.V. and Croce, C.M. (2009) At least ten genes define the imprinted Dlk1–Dio3 cluster on mouse chromosome 12qF1. PLoS One 4, e4352.
[7] Seitz, H., Royo, H., Bortolin, M.L., Lin, S.P., Ferguson-Smith, A.C. and Cavaille, J. (2004) A large imprinted microRNA gene cluster at the mouse Dlk1-Gtl2 domain. Genome Res. 14, 1741–1748.
[8] Cavaille, J., Seitz, H., Paulsen, M., Ferguson-Smith, A.C. and Bachellerie, J.P. (2002) Identification of tandemly-repeated C/D snoRNA genes at the imprinted human 14q32 domain reminiscent of those at the Prader-Willi/Angelman syndrome region. Hum. Mol. Genet. 11, 1527–1538.
[9] Schmidt, J.V., Matteson, P.G., Jones, B.K., Guan, X.J. and Tilghman, S.M. (2000) The Dlk1 and Gtl2 genes are linked and reciprocally imprinted. Genes Dev. 14, 1997–2002.
[10] Kircher, M., Bock, C. and Paulsen, M. (2008) Structural conservation versus functional divergence of maternally expressed microRNAs in the Dlk1/Gtl2 imprinting region. BMC Genomics 9, 346.
[11] Stadtfeld, M. et al. (2010) Aberrant silencing of imprinted genes on chromosome 12qF1 in mouse induced pluripotent stem cells. Nature 465, 175–181.
[12] Liu, L. et al. (2010) Activation of the imprinted Dlk1–Dio3 region correlates with pluripotency levels of mouse stem cells. J. Biol. Chem. 285, 19483–19490.
[13] Stadtfeld, M. et al. (2012) Ascorbic acid prevents loss of Dlk1–Dio3 imprinting and facilitates generation of all-iPS cell mice from terminally differentiated B cells. Nat. Genet. 44 (398–405), S1–S2.
[14] Takada, S., Paulsen, M., Tevendale, M., Tsai, C.E., Kelsey, G., Cattanach, B.M. and Ferguson-Smith, A.C. (2002) Epigenetic analysis of the Dlk1-Gtl2 imprinted domain on mouse chromosome 12: implications for imprinting control from comparison with Igf2-H19. Hum. Mol. Genet. 11, 77–86.
[15] Hiura, H., Komiyama, J., Shirai, M., Obata, Y., Ogawa, H. and Kono, T. (2007) DNA methylation imprints on the IG-DMR of the Dlk1-Gtl2 domain in mouse male germline. FEBS Lett. 581, 1255–1260.
[16] Lin, S.P., Youngson, N., Takada, S., Seitz, H., Reik, W., Paulsen, M., Cavaille, J. and Ferguson-Smith, A.C. (2003) Asymmetric regulation of imprinting on the maternal and paternal chromosomes at the Dlk1-Gtl2 imprinted cluster on mouse chromosome 12. Nat. Genet. 35, 97–102.
[17] Nowak, K., Stein, G., Powell, E., He, L.M., Naik, S., Morris, J., Marlow, S. and Davis, T.L. (2011) Establishment of paternal allele-specific DNA methylation at the imprinted mouse Gtl2 locus. Epigenetics 6, 1012–1020.
[18] Sato, S., Yoshida, W., Soejima, H., Nakabayashi, K. and Hata, K. (2011) Methylation dynamics of IG-DMR and Gtl2-DMR during murine embryonic and placental development. Genomics 98, 120–127.
[19] Donsante, A., Miller, D.G., Li, Y., Vogler, C., Brunt, E.M., Russell, D.W. and Sands, M.S. (2007) AAV vector integration sites in mouse hepatocellular carcinoma. Science 317, 477.
[20] Wang, P.R., Xu, M., Toffanin, S., Li, Y., Llovet, J.M. and Russell, D.W. (2012) Induction of hepatocellular carcinoma by in vivo gene targeting. Proc. Natl. Acad. Sci. U.S.A. 109, 11264–11269.
[21] Dupuy, A.J. et al. (2009) A modified sleeping beauty transposon system that can be used to model a wide variety of human cancers in mice. Cancer Res. 69, 8150–8156.
[22] Riordan, J.D. et al. (2013) Identification of rtl1, a retrotransposon-derived imprinted gene, as a novel driver of hepatocarcinogenesis. PLoS Genet. 9, e1003441.
[23] Dindot, S.V., Person, R., Strivens, M., Garcia, R. and Beaudet, A.L. (2009) Epigenetic profiling at mouse imprinted gene clusters reveals novel epigenetic and genetic features at differentially methylated regions. Genome Res. 19, 1374–1383.
[24] Takai, D. and Jones, P.A. (2003) The CpG island searcher: a new WWW resource. In Silico Biol. 3, 235–240.
[25] Hackett, J.A. and Surani, M.A. (2013) DNA methylation dynamics during the mammalian life cycle. Philos. Trans. R. Soc. Lond. B Biol. Sci. 368, 20110328.
[26] Seisenberger, S., Peat, J.R., Hore, T.A., Santos, F., Dean, W. and Reik, W. (2013) Reprogramming DNA methylation in the mammalian life cycle: building and breaking epigenetic barriers. Philos. Trans. R. Soc. Lond. B Biol. Sci. 368, 20110330.
[27] McMurray, E.N. and Schmidt, J.V. (2012) Identification of imprinting regulators at the Meg3 differentially methylated region. Genomics 100, 184–194.
[28] Bell, A.C. and Felsenfeld, G. (2000) Methylation of a CTCF-dependent boundary controls imprinted expression of the Igf2 gene. Nature 405, 482–485.
[29] Kurukuti, S. et al. (2006) CTCF binding at the H19 imprinting control region mediates maternally inherited higher-order chromatin conformation to restrict enhancer access to Igf2. Proc. Natl. Acad. Sci. U.S.A. 103, 10684–10689.
[30] Yoon, B. et al. (2005) Rasgrf1 imprinting is regulated by a CTCF-dependent methylation-sensitive enhancer blocker. Mol. Cell. Biol. 25, 11184–11190.
[31] Fitzpatrick, G.V., Pugacheva, E.M., Shin, J.Y., Abdullaev, Z., Yang, Y., Khatod, K., Lobanenkov, V.V. and Higgins, M.J. (2007) Allele-specific binding of CTCF to the multipartite imprinting control region KvDMR1. Mol. Cell. Biol. 27, 2636–2647.
[32] Phillips, J.E. and Corces, V.G. (2009) CTCF: master weaver of the genome. Cell 137, 1194–1211.
[33] ENCODE (2012) An integrated encyclopedia of DNA elements in the human genome. Nature 489, 57–74.
[34] Wang, H. et al. (2012) Widespread plasticity in CTCF occupancy linked to DNA methylation. Genome Res. 22, 1680–1688.
[35] Karolchik, D. et al. (2013) The UCSC genome browser database: 2014 update. Nucleic Acids Res.
[36] Ziebarth, J.D., Bhattacharya, A. and Cui, Y. (2013) CTCFBSDB 2.0: a database for CTCF-binding sites and genome organization. Nucleic Acids Res. 41, D188–D194.
[37] Gagne, A., Hochman, A., Qureshi, M., Tong, C., Arbon, J., McDaniel, K. and Davis, T.L. (2014) Analysis of DNA methylation acquisition at the imprinted Dlk1 locus reveals asymmetry at CpG dyads. Epigenetics Chromatin 7, 9.
[38] Lin, S.P., Coan, P., da Rocha, S.T., Seitz, H., Cavaille, J., Teng, P.W., Takada, S. and Ferguson-Smith, A.C. (2007) Differential regulation of imprinting in the murine embryo and placenta by the Dlk1–Dio3 imprinting control region. Development 134, 417–426.
[39] Takahashi, N., Okamoto, A., Kobayashi, R., Shirai, M., Obata, Y., Ogawa, H., Sotomaru, Y. and Kono, T. (2009) Deletion of Gtl2, imprinted non-coding RNA, with its differentially methylated region induces lethal parent-origin-dependent defects in mice. Hum. Mol. Genet. 18, 1879–1888.
[40] Kang, K., Chung, J.H. and Kim, J. (2009) Evolutionary conserved motif finder (ECMFinder) for genome-wide identification of clustered YY1- and CTCF-binding sites. Nucleic Acids Res. 37, 2003–2013.